Bond Behavior of Concrete-Filled Steel Tube (CFT) Structures

JIE ZHANG, MARK D. DENAVIT, JEROME F. HAJJAR and XILIN LU

ABSTRACT

To achieve internal force transfer while avoiding the use of steel stud anchors or a bearing mechanism within concrete-filled steel tubes (CFTs), an accurate assessment of the bond strength of CFTs is required. However, calculation of the bond within CFTs remains a challenging problem due to lack of a general procedure that can account for the range of connection configurations seen within composite construction. A new approach for assessing the nominal bond strength for both rectangular and circular CFTs is proposed. Based on the results of push-out experiments of CFTs, the nominal bond stress is shown to vary with tube shape and dimensions, and formulas are proposed to capture this behavior. The longitudinal bond transfer length is derived by examining the distribution of bond stress along the height of the column as well as experimental data from CFT connection tests. The circumferential bond transfer width is identified as the entire perimeter of the interface, accounting for the contribution to the bond strength from the interface on the sides that do not have girders or braces framing in. The resulting nominal bond strength is then shown to have a resistance factor of 0.45 for load and resistance factor design (LRFD) and safety factor of 3.33 for allowable strength design (ASD).

Keywords: concrete-filled steel tubes, composite action, connections, bond strength, critical bond stress, slip.

INTRODUCTION

Composite braced or unbraced frame structures that use concrete-filled steel tube (CFT) columns provide superior performance when subjected to nonseismic and seismic lateral loading. This has led to a continued increase in the use of these members in the primary lateral-resistance systems of structures. Steel tubes serve as the formwork for concrete placement, potentially expediting construction and reducing cost (Bridge and Webb, 1993). In addition, the composite action of the steel tube and concrete core can effectively delay the buckling of steel tubes and significantly increase the ductility of the concrete core. To ensure these beneficial effects, it is important to have a comprehensive understanding of the composite action between the constituent materials, particularly in critical connection regions where load is transferred to the CFT column from girders or braces. If the steel tube cannot effectively transfer the axial forces to the concrete, the resulting localized stresses may lead to premature yielding or local buckling of the steel tube. Therefore, the bond transfer mechanisms need to be accurately assessed and incorporated into the design. Transfer of stress through natural bond, without the use of steel stud anchors or a bearing mechanism, is often the most economical connection detail; however, efforts to characterize the bond strength are hindered by varying experimental results, even among like specimens (Roeder et al., 1999).

The design provisions for load transfer in CFTs through direct bond in the AISC *Specification for Structural Steel Buildings* (AISC, 2010) are based predominantly on the results of push-out and push-off tests. Using only these data, there is little quantitative evidence to support the effective transfer area because these experimental configurations do not share the same loading and boundary conditions as typical composite columns. Thus, further investigation into bond behavior is important to ascertain a more accurate prediction on the bond strength of CFTs in the design provisions. In this work, a new formula for nominal bond strength is proposed. Nominal bond strength, longitudinal bond transfer length, circumferential bond transfer width and resistance and safety factors are examined separately.

EXISTING DESIGN PROVISIONS

The nominal bond strength of rectangular (RCFT) and circular concrete filled-steel tubes (CCFT) prescribed in the AISC *Specification* (AISC, 2010) is given as:

(a) For RCFT:

$$R_n = B^2 C_{in} F_{in} \tag{1}$$

Jie Zhang, Ph.D., Assistant Chief Engineer, Jiading MTR Construction and Investment Co. Ltd., Shanghai, China. E-mail: jiezhang000@gmail.com

Mark D. Denavit, Graduate Research Assistant, Department of Civil and Environmental Engineering, University of Illinois at Urbana-Champaign, Urbana, IL. E-mail: denavit2@illinois.edu

Jerome F. Hajjar, Ph.D., P.E., Professor and Chair, Department of Civil and Environmental Engineering, Northeastern University, Boston, MA (corresponding author). E-mail: jf.hajjar@neu.edu

Xilin Lu, Ph.D., Cheung Kong Scholars Professor, Tongji University, Shanghai, China. E-mail: lxlst@tongji.edu.cn

(b) For CCFT:

$$R_n = 0.25\pi D^2 C_{in} F_{in} \quad (2)$$

where

C_{in} = 2 if the CFT extends to one side of the point of force transfer
= 4 if the CFT extends to both sides of the point of force transfer
R_n = nominal bond strength, kips
F_{in} = nominal bond stress = 60 psi
B = overall width of rectangular steel section along face transferring load, in.
D = outside diameter of the round steel section, in.

This formula can be seen as the product of three values: the nominal bond stress, F_{in}; the circumferential bond transfer width, B for RCFT and $0.25\pi D$ for CCFT; and the longitudinal bond transfer length, BC_{in} for RCFT and DC_{in} for CCFT. The nominal bond stress, F_{in}, is taken as 60 psi (0.4 MPa). This value is seen as a reasonable lower bound of bond stresses observed in experimental results, mostly consisting of push-out tests (AISC, 2010). The bond length is dependent on the value of C_{in}, which is equal to 2 if CFT extends to only one side of the point of force transfer (e.g., the top or bottom story) and 4 if the CFT extends both sides. The bond width is computed assuming only the face to which load is applied for RCFT, or one-quarter of the perimeter for CCFT is active in transferring stress. The resistance factor, ϕ, is given as 0.45 and safety factor, Ω, is given as 3.33 based on an examination of push-off test results from Morishita et al. (1979a, 1979b).

The European model building code (CEN, 2004) also provides provisions relating to transfer strength by direct bond. A differentiation is made in the bond stress based on the shape of the steel tube: 60 psi (0.40 MPa) for RCFT and 80 psi (0.55 MPa) for CCFT. The bond transfer length is limited to the lesser of twice the minimum transverse dimension of the column, or one-third the column length. No mention is given to the bond transfer width, so it may be assumed that the full perimeter is engaged in the load transfer. It is noted that for a RCFT column with two girders framing in, the nominal bond strength, as calculated by the AISC *Specification* and Eurocode, is the same.

Tomii (1985) highlights a design procedure from the Japanese code in which a lower bond strength and larger bond transfer area are used. For long-term loading, the bond strength is 14 psi (0.10 MPa) for RCFT and 21 psi (0.15 MPa) for CCFT. The bond length is taken as the distance from the mid-height of the upper column to the mid-height of the lower column, and the bond width is taken as the full perimeter of the steel–concrete interface.

Other procedures have been proposed to characterize bond strength for design. Roeder et al., (1999) examined results from push-out tests on CCFTs and found a correlation between bond strength and the cross-sectional dimensions of the tube. A linear equation was proposed to describe the bond stress as a function of the D/t ratio. The linear equation implied that no reliable bond stress could be obtained for CCFTs with a D/t ratio greater than 80. Two checks are proposed using this bond stress. First, at the ultimate load level, the bond stress is applied around the entire perimeter and along a length equal to the lesser of length of the column, or 3.5 times the diameter of the steel tube. Second,

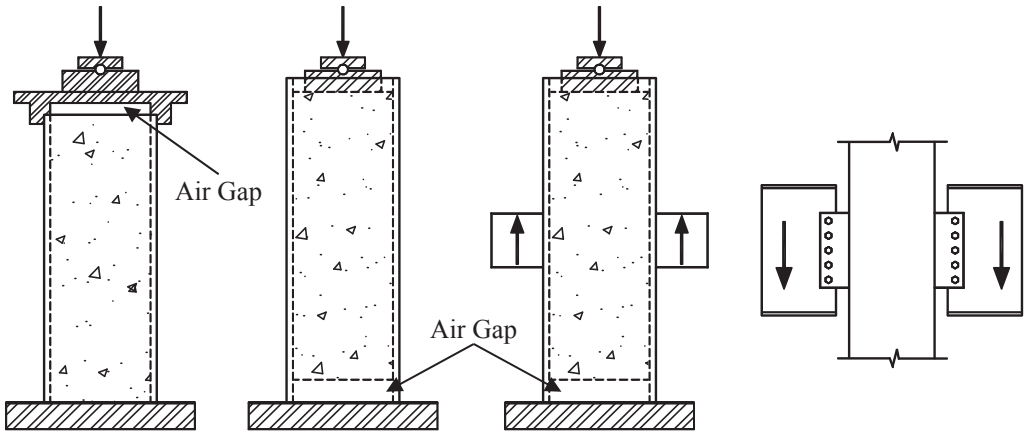

Fig. 1. Typical CFT test configurations to assess bond behavior.

noting evidence of cyclic deterioration of bond strength, at the serviceability level, the bond strength is computed using a triangular stress distribution over a length of one-half the tube diameter.

Variation in the bond stress based on tube dimensions was also observed for RCFTs by Parsley et al. (2000). A formula for bond strength was proposed as a linear function of the slenderness parameter t/H^2.

EXPERIMENTAL STUDIES

Experimental studies on bond behavior of CFT members have most frequently been conducted through the use of push-out tests (Virdi and Dowling, 1980; Shakir-Khalil, 1991, 1993b, 1993c; Roeder et al., 1999; Parsley et al., 2000; Xu et al., 2009; Aly et al., 2010; Yin and Lu, 2010), push-off tests (Morishita et al., 1979a, 1979b; Tomii et al., 1980a, 1980b), or connection tests (Dunberry et al., 1987; Shakir-Khalil, 1993a, 1993d, 1994a, 1994b; Shakir-Khalil and Al-Rawdan, 1995). Each of these types of tests (see Figure 1) has advantages and disadvantages in the assessment of the natural bond strength of CFTs. The boundary conditions of push-out tests (Figures 1b and 1c) induce constant bond stress at the ultimate limit state and thus provide little information as to the distribution of bond stress over the length along the column. However, in push-off and connection tests, where the bond stress is not constant, it is difficult to accurately estimate the magnitude of stress. In typical push-out and push-off tests, the specimen bears directly on a rigid support at the base (Figure 1b), excluding the beneficial effects that a shear connection provides. Push-out tests where force is applied to the concrete core and resisted by shear tabs attached to the steel tube (Figure 1c) and connection tests (Figure 2) include these beneficial effects and thus provide the closest analogs to typical shear connections (or other connection types that feature eccentric introduction of force into the CFT) used in practice.

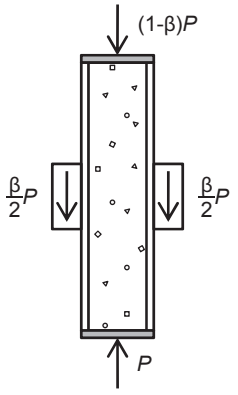

Fig. 2. CFT connection test schematic.

CFT Push-Out Tests without Shear Tabs

Critical bond stresses from push-out test results are computed by dividing the peak load attained during the test by the entire area of the steel–concrete interface. The resistance observed in these tests has been generally attributed to three primary mechanisms: adhesion, friction and wedging (Parsley et al., 2000; Johansson 2003). Adhesion, provided by the chemical bond between the concrete and steel, is a brittle mechanism and is only active at most during the early stages of load. It may not be active at all depending on the relative amplitudes of radial enlargement of the steel tube caused by the wet concrete, shrinkage of the concrete and the roughness of the steel tube (Roeder et al., 1999). Friction is the product of the roughness of the steel–concrete interface and the contact pressure existing at the interface. Wedging occurs as the motion of the concrete core is resisted by geometric irregularities in the steel tube.

Bond stresses obtained from push-out tests are highly variable and found to range over two orders of magnitude. However, some noticeable trends have been identified (Roeder et al., 1999; Parsley et al., 2000). The bond stress for CCFTs is larger than for RCFTs. Tube dimensions have an effect on the results, with lower bond stress obtained for larger and more slender tubes. The surface preparation of the interior of the steel tube and the shrinkage/expansive potential of the concrete have also been shown to have an influence on the bond stress. Concrete and steel material strengths, however, appear to have no consistent effect on the bond stress. Eccentric loading of the column has also been shown to have a beneficial effect on the bond stress. This increase is so significant that it has been suggested that a bond need not be checked in the presence of significant bending moments in the column (Roeder et al., 2009). This paper does not specifically address the effect of eccentrically loaded columns, rather concentrating on the worst-case concentric loading.

Details of push-out tests without shear tabs reported in the literature are presented in Table 1 for RCFTs and Table 2 for CCFTs. All specimens from each reference were included, with the exception of those with shear tabs, those with mechanical shear connecters, those where the steel-concrete interface was manipulated by machining or applying a lubricant, those where the load was applied eccentrically or those with expansive concrete. Specimens that were loaded cyclically were included in the table because they represent loading conditions that typical connections may experience, and they did not significantly skew the results of the analysis.

CFT Push-Out Tests with Shear Tabs

Assessing bond stress based on the results of typical push-out and push-off tests neglects beneficial effects that occur in typical beam-to-column connections due to the rotation

Table 1. RCFT Push-Out Tests without Shear Tabs								
Reference	Number of Specimens	L (in.)	H, B (in.)	t (in.)	H/t, B/t	F_y (ksi)	f'_c (ksi)	F_{in} (psi)
Shakir-Khalil, 1991	6	16	3.1–5.9	0.20	16–30	43.0	5.7–6.3	29–193
Shakir-Khalil, 1993a	6	8–24	5.9	0.20	30	43.0	5.9	48–86
Shakir-Khalil, 1993b	2	16	5.9	0.20	30	43.0	5.7	29
Parsley et al., 2000	4	48–60	8.0–10.0	0.25	32–40	48.0	5.9–6.6	25–42

Table 2. CCFT Push-Out Tests without Shear Tabs								
Reference	Number of Specimens	L (in.)	D (in.)	t (in.)	D/t	F_y (ksi)	f'_c (ksi)	F_{in} (psi)
Virdi and Dowling, 1975	82	6–18	5.7–12.0	0.20–0.40	15–32	mild steel	3.2–6.7	75–431
Shakir-Khalil, 1991	2	16	6.6	0.20	34	43.0	6.5	63–69
Shakir-Khalil, 1993a	6	8–24	6.6	0.20	34	43.0	6.1	95–134
Shakir-Khalil, 1993b	2	16	6.6	0.20	34	43.0	6.5	63–69
Roeder et al., 1999	18	30–76	10.8–24.0	0.22–0.53	20–109	not given	4.0–6.9	1.5–114
Xu et al., 2009	3	20	6.1–6.3	0.11–0.18	35–56	not given	6.8	87–97
Aly et al., 2010	14	16	4.5	0.13	36	50.8	5.9–13.2	51–181

of the shear tabs (or similar eccentricities that may occur for introduction of force between a girder and the steel tube in the connection topology) (Johansson, 2003). The rotation of the shear tab during loading results in pinching of the concrete core where the shear tab rotates inward and constriction of the steel tube where the shear tab rotates outward (Figure 3). Both cases result in increased contact pressure between the steel and concrete and thus greater frictional resistance to slip.

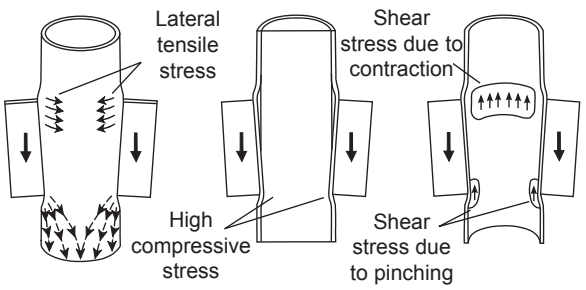

Fig. 3. Increased contact force with shear tab rotation (adapted from Johansson, 2003).

Push-out tests where load was applied to the steel tube through shear tabs have been reported in the literature (Shakir-Khalil, 1993c; Parsley et al., 2000). Details of these experiments are presented in Table 3 for RCFTs and Table 4 for CCFTs.

The failure mode of the all of the RCFT specimens was slip. A typical load-slip relationship shows a high initial stiffness up to the peak load. Many specimens showed a sharp decrease in strength following the peak load, while others maintained a load near the peak load. Two specimens (G2 and G3) displayed a steadily increasing load following a reduction in stiffness near the peak load of other similar specimens. In all cases, $P_{applied}$ was taken as the peak load attained during the test. The average bond stress, F_{in}, for the full set of RCFT tests is 93 psi. The average bond stress for specimens where the shear tabs were located near mid-height of the column is 118 psi, while it is 53 psi for specimens with shear tabs near the column ends.

Only some of the CCFT specimens failed due to slip. Specimens D1a, D1b, F1a and F1b (Shakir-Khalil, 1993c)

Table 3. RCFT Push-Out Tests with Shear Tabs									
Reference	Specimen	L (in.)	$H = B$ (in.)	t (in.)	H/t	F_y (ksi)	f'_c (ksi)	$P_{applied}$ (kip)	F_{in} (psi)
Shakir-Khalil, 1993c	C1a	15.6	5.91	0.197	30.0	39.9	6.2	38.1	110.5
	C1b	15.6	5.91	0.197	30.0	39.9	6.2	51.5	149.5
	C2a	15.7	5.91	0.197	30.0	39.9	6.2	51.5	148.4
	C2b	15.7	5.91	0.197	30.0	39.9	6.2	53.1	153.3
	E1a	15.7	7.87	0.248	31.7	39.9	6.6	37.5	81.0
	E1b	15.7	7.87	0.248	31.7	39.9	6.6	18.0	38.7
	G2	15.8	5.91	0.197	30.0	39.9	6.5	44.7	128.2
	G3	15.9	5.91	0.197	30.0	39.9	6.5	47.0	133.7
	G4	15.8	5.91	0.197	30.0	39.9	6.5	23.4	67.0
Parsley et al., 2000	CFT2	48.0	8.00	0.228	35.1	48.0	6.6	98.0	67.7
	CFT5	48.0	8.00	0.228	35.1	48.0	6.6	101.0	69.7
	CFT8	58.5	10.00	0.232	43.1	48.0	5.9	67.0	30.0
	CFT6	58.5	10.00	0.234	42.7	48.0	5.9	70.0	31.4
								Average:	93.0
								Std. Dev.:	46.4

Table 4. CCFT Push-Out Tests with Shear Tabs									
Reference	Specimen	L (in.)	D (in.)	t (in.)	D/t	F_y (ksi)	f'_c (ksi)	$V_{applied}$ (kip)	F_{in} (psi)
Shakir-Khalil, 1993c	D1a	15.7	6.63	0.197	33.7	39.9	6.2	186.6	605
	D1b	15.7	6.63	0.197	33.7	39.9	6.2	182.1	594
	F1a	15.8	6.63	0.197	33.7	39.9	6.1	212.9	689
	F1b	15.6	6.63	0.197	33.7	39.9	6.6	218.3	715
	H2	15.8	6.63	0.197	33.7	39.9	6.5	172.0	556
	H3	15.9	6.63	0.197	33.7	39.9	6.5	167.0	538
	H4	15.7	6.63	0.197	33.7	39.9	6.5	60.5	196
								Average:	556
								Std. Dev.:	172

achieved higher-than-expected strengths, and the shear tabs failed prior to slip. In an analysis of one of these specimens, Johansson (2003) identified the rotation of the shear tabs and the increased contact forces to be the cause of the unexpectedly high bond strength. The failure mode of specimens H2 and H3 was slip; however, no peak load was observed because the load was seen to steadily increase. One specimen, H4, failed through slip and displayed a peak load. Again, in all cases, $P_{applied}$ was taken as the peak load attained during the test. The bond stress for CCFTs is much larger than for RCFTs, with an average applied bond stress, F_{in}, of 556 psi. However, this value is unreasonably high for design purposes, because it was achieved only for a few similarly proportioned tests and may not be indicative of expected behavior for the variety of configurations expected in practice.

Nominal Bond Stress

Push-out tests, whether with or without shear tabs, provide a direct means of assessing the bond stress. Trends in the push-out test results that have been identified include the dependence of the bond stress on factors not typically known at the time of design (e.g., the condition of the steel–concrete

surface and the shrinkage/expansive potential of the concrete). For a bond stress formula intended for design, these factors should thus be included in an average sense rather than explicitly. Among the strongest trends identified is the dependence of the bond stress on tube dimensions. Roeder et al., (1999) proposed a formula for bond stress of CCFTs based on the D/t ratio. Parsley et al., (2000) proposed a formula for bond stress of RCFTs based on t/H^2. The ratio t/H^2 was selected based on a mechanistic analysis; it is proportional to the radial stiffness of cylindrical, thin-walled pressure vessels.

It is noted that there is insufficient experimental evidence to determine which of the two transverse dimensions of an RCFT cross-sections—i.e., the width or the height—should be used for determining bond stress because most of the RCFT push-out tests (Tables 1 and 3) had square sections. The height, defined here as the longer transverse dimension, was selected as the conservative choice, but further investigation is appropriate for sections with a high aspect ratio (H/B).

The results of push-out tests are plotted in Figure 4 against both of these parameters. All push-out tests from Tables 1 through 4 were included. The bond stress is typically higher for push-out tests with shear tabs, showing the

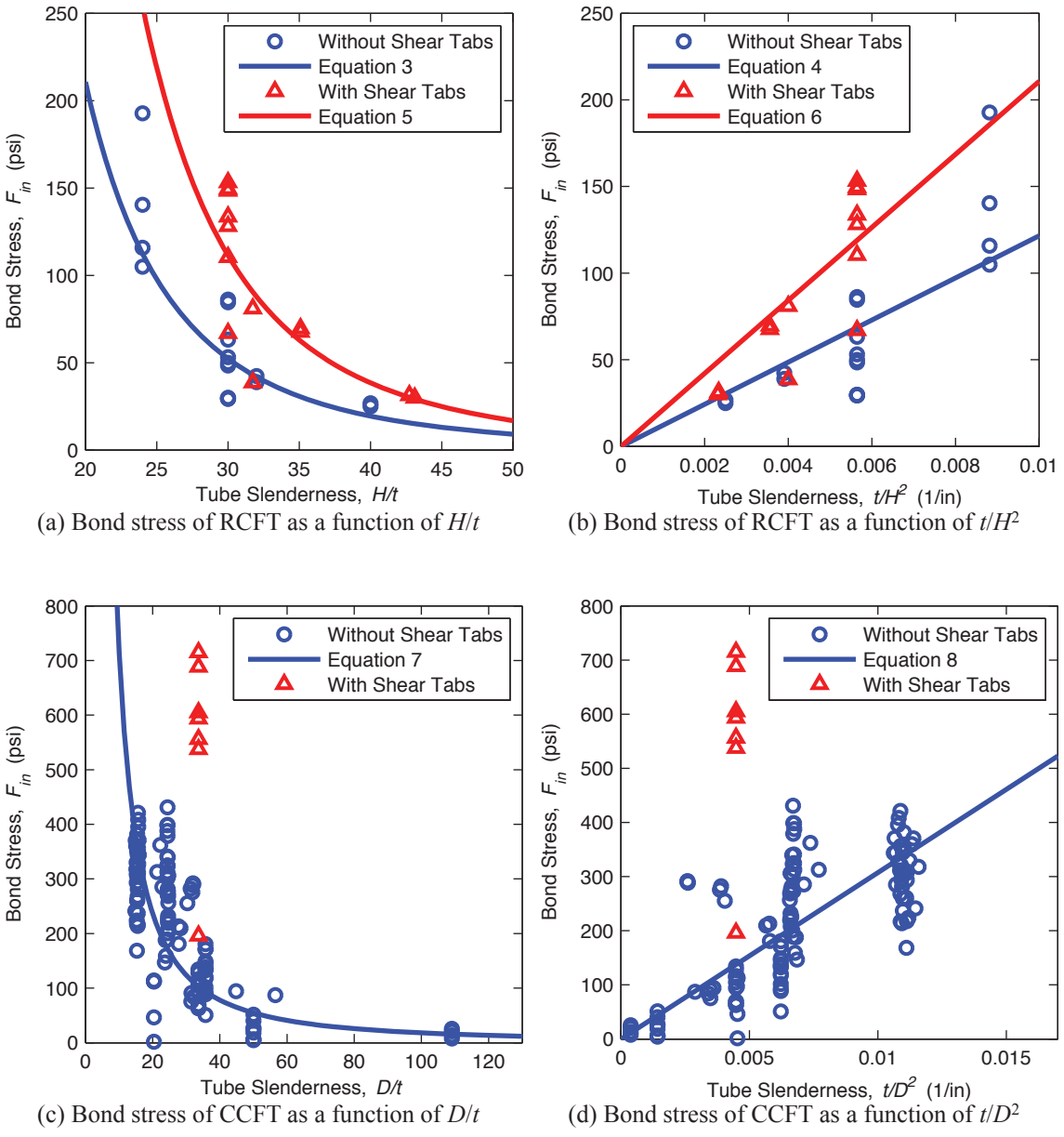

(a) Bond stress of RCFT as a function of H/t

(b) Bond stress of RCFT as a function of t/H^2

(c) Bond stress of CCFT as a function of D/t

(d) Bond stress of CCFT as a function of t/D^2

Fig. 4. Bond stress for CFT as a function of tube slenderness.

beneficial effects rotation of the shear tab has on bond stress. As seen in Figure 4, there is significant variation in the bond stress, indicating that the constant values used in current design methodologies are insufficient, especially for thin tubes and large cross-sections where the bond stress may be overestimated.

To obtain a design formula, a least squares curve fit can be made to these data. The forms of the equations chosen were selected to provide a good fit to the available data, have reasonable bounds, and produce non-negative bond stress values. The results of the regression analysis are as follows:

RCFT push-out tests without shear tabs:

$$F_{in} = 6.23\times10^{6}\left(H/t\right)^{-3.44} \quad R^2 = 0.68 \tag{3}$$

$$F_{in} = 12{,}100\left(t/H^2\right) \quad R^2 = 0.56 \tag{4}$$

RCFT push-out tests with shear tabs:

$$F_{in} = 3.23\times10^{7}\left(H/t\right)^{-3.70} \quad R^2 = 0.61 \tag{5}$$

$$F_{in} = 21{,}100\left(t/H^2\right) \quad R^2 = 0.66 \tag{6}$$

CCFT push-out tests without shear tabs:

$$F_{in} = 28{,}500\left(D/t\right)^{-1.59} \quad R^2 = 0.33 \tag{7}$$

$$F_{in} = 30{,}700\left(t/D^2\right) \; R^2 = 0.50 \tag{8}$$

where F_{in} is in psi and t, H, and D are in inches.

A curve fit was not performed for CCFT push-out tests with shear tabs because all the available tests had nearly the same size tube. The two different functions for each case represent the two different parameters (e.g., H/t and t/H^2) chosen to represent the tube dimensions. In addition to accuracy, quantified by the R^2 value associated with each formula, the formulas can be judged by their usability. Based on these criteria, the formulas based on t/D^2 and t/H^2 are recommended for design. Furthermore, the formulas computed with the data from the push-out tests without shear tabs are recommended for design because they provide a lower bound for the behavior expected in typical shear connections and allow for the greatest consistency between tube shapes. Thus Equation 4 is recommended for the nominal bond stress of RCFTs, and Equation 8 is recommended for CCFTs. Both of these formulas have no upper bound on the bond stress, though one could be implemented based on the results of the stockiest tubes for each shape (i.e., 100 to 200 psi for RCFTs and 200 to 400 psi for CCFTs).

CFT Connection Tests

Push-out tests have explicit boundary conditions and paths for load transfer and thus are well suited for an assessment of bond stress; however, they provide little evidence of the bond length or bond width of typical connections. Column connection tests that are instrumented to measure load transfer such as those conducted by Dunberry et al. (1987), Shakir-Khalil (1993a and d, 1994a and b) and Shakir-Khalil and Al-Rawdan (1995) provide a means to quantify the area over which a nominal bond stress acts in typical connections. A schematic of the test specimens and loading is presented in Figure 2. Shear tabs are welded to the outside of the steel tubes to transfer the eccentric shears through the interfaces. Load is applied at both column ends and at the shear connections, in a ratio described by β.

The experimental strength of all of these specimens was near the squash load, indicating that limit states other than cross-sectional strength, including slip, either did not have a significant effect on the strength or did not occur. In the tests performed by Dunberry et al. (1987), local buckling was a typical failure mode. The local buckling occurred near the connection for some specimens, indicating that the loading conditions possibly had an influence on the strength—and away from the connection for other specimens. A strain incompatibility was observed in the connection region, which extended approximately three tube widths below the connection and one to two tube widths above the connection. The concrete load steadily rose in this region, indicating a load was transferred along its length, although the rise was steepest in the bottom half of the connection, indicating that pinching due to rotation of the shear tabs played a significant role in transferring the load. The tests performed by Shakir-Khalil (1993a and d, 1994a and b) and Shakir-Khalil and Al-Rawdan (1995) displayed somewhat similar behavior. The typical failure mode was overall collapse of the column without indication of a detrimental effect on the strength from slip. The observed transfer length was shorter than that observed by Dunberry et al. (1987), as strains equalized within a tube width above and below the connection.

Additional details of the experiments are shown in Table 5 for RCFTs and in Table 6 for CCFTs. The tabulated applied load, $P_{applied}$, is the total load applied to the steel tube in the connection region. This load is not necessarily indicative of the slip strength because many of the specimens failed away from the connection region or the strength was not reached due to test rig limitations. Nonetheless, these specimens were included in the table because they provide a lower

Table 5. RCFT Connection Tests

Reference	Specimen	L (in.)	$H=B$ (in.)	t (in.)	H/t	F_y (ksi)	f'_c (ksi)	β	$P_{applied}$ (kip)	$V'_{applied}$ (kip)	Number of Girders	$R_{n,AISC2010}$ (kip)	Test-to-Predicted	F_{in} (Eq. 6) (psi)	$L_{transfer}$ (in.)	$L_{transfer}/H$
Dunberry et al., 1987	A1	118.1	4.01	0.193	20.8	53.7	3.6	1.00	186.6	38.2	2	7.73	4.9	252.9	10.41	2.6
	A2	118.1	4.99	0.187	26.7	51.3	3.6	1.00	200.8	52.9	2	11.96	4.4	158.3	18.08	3.6
	A3	118.1	5.00	0.189	26.5	51.3	3.6	0.50	130.4	34.1	2	11.98	2.8	159.4	11.59	2.3
	A4	118.1	4.98	0.187	26.7	51.3	3.6	0.30	81.7	21.5	2	11.89	1.8	159.0	7.35	1.5
	B1	118.1	7.02	0.244	28.7	56.3	2.5	0.30	142.7	28.1	2	23.65	1.2	104.7	10.28	1.5
	B2	118.1	7.01	0.189	37.1	51.2	2.5	0.45	172.0	45.3	2	23.60	1.9	81.1	21.05	3.0
	B3	118.1	8.01	0.246	32.5	57.9	2.5	0.30	180.6	38.9	2	30.78	1.3	81.0	15.96	2.0
	C1	59.1	4.01	0.190	21.1	54.2	3.5	1.00	198.1	39.6	2	7.71	5.1	249.3	10.94	2.7
	D1	78.7	6.00	0.190	31.6	64.3	4.3	0.50	201.3	58.1	2	17.28	3.4	111.5	23.20	3.9
	D2	78.7	6.00	0.189	31.8	64.3	4.3	0.50	203.0	59.0	2	17.30	3.4	110.4	23.76	4.0
	D3	78.7	6.00	0.189	31.7	64.3	4.3	0.50	210.8	61.1	2	17.30	3.5	110.8	24.49	4.1
	D4	78.7	6.00	0.189	31.8	64.3	4.3	0.50	199.6	57.9	2	17.30	3.3	110.6	23.28	3.9
Shakir-Khalil, 1993d, 1994a, 1994b	B1	110.2	5.91	0.197	30.0	47.6	5.6	0.20	59.5	23.9	2	16.74	1.4	119.1	9.10	1.5
	B3	110.2	5.91	0.197	30.0	49.3	5.5	0.29	87.0	34.1	2	16.74	2.0	119.1	12.97	2.2
	B5	110.2	5.91	0.197	30.0	47.6	5.9	0.20	57.2	23.9	2	16.74	1.4	119.1	9.08	1.5
	B7	110.2	5.91	0.197	30.0	47.4	5.7	0.29	79.0	32.4	2	16.74	1.9	119.1	12.34	2.1
	D1	110.2	7.87	0.248	31.7	47.4	6.6	0.20	133.5	61.2	2	29.76	2.1	84.4	24.55	3.1
	D2	110.2	7.87	0.248	31.7	60.2	6.5	0.20	130.7	52.2	2	29.76	1.8	84.4	20.96	2.7
	E1	110.2	5.91	0.197	30.0	53.3	6.5	0.20	71.9	29.7	2	16.74	1.8	119.1	11.32	1.9
	E2	110.2	5.91	0.197	30.0	53.5	6.2	0.29	105.6	42.4	2	16.74	2.5	119.1	16.13	2.7
	E3	110.2	5.91	0.197	30.0	53.5	5.7	0.20	68.5	25.9	2	16.74	1.5	119.1	9.88	1.7
	E4	110.2	5.91	0.197	30.0	53.3	5.3	0.29	96.3	34.8	2	16.74	2.1	119.1	13.27	2.2
	E5	110.2	5.91	0.197	30.0	53.3	5.1	0.20	72.1	25.6	2	16.74	1.5	119.1	9.74	1.6
	E6	110.2	5.91	0.197	30.0	52.9	5.5	0.29	97.1	36.4	2	16.74	2.2	119.1	13.86	2.3
	E7	110.2	5.91	0.197	30.0	53.3	5.9	0.20	68.7	26.8	2	16.74	1.6	119.1	10.20	1.7
	E8	110.2	5.91	0.197	30.0	52.9	5.7	0.29	98.3	37.5	2	16.74	2.2	119.1	14.27	2.4
Shakir-Khalil & Al-Rawdan, 1995	F1	110.2	5.91	0.197	30.0	47.9	5.3	0.17	44.9	17.5	1	8.37	2.1	119.1	6.67	1.1
	F2	110.2	5.91	0.197	30.0	47.9	6.6	0.11	33.9	15.0	1	8.37	1.8	119.1	5.71	1.0
	F3	110.2	5.91	0.197	30.0	48.2	6.3	0.17	43.8	18.7	1	8.37	2.2	119.1	7.13	1.2
	F4	110.2	5.91	0.197	30.0	48.2	6 .5	0.11	33.2	14.6	1	8.37	1.7	119.1	5.54	0.9

Table 6. CCFT Connection Tests																
Reference	Specimen	L (in.)	D (in.)	t (in.)	D/t	F_y (ksi)	f'_c (ksi)	β	$P_{applied}$ (kip)	$V'_{applied}$ (kip)	Number of Girders	$R_{n,AISC2010}$ (kip)	Test-to-Predicted	F_{in} (Eq. 8) (psi)	$L_{transfer}$ (in.)	$L_{transfer}/D$
Shakir-Khalil, 1993a, 1994a	A1	110.2	6.63	0.197	33.7	46.4	6.2	0.20	61.9	30.5	2	16.55	1.8	137.6	11.31	1.7
	A2	110.2	6.63	0.197	33.7	46.8	6.5	0.20	57.7	29.0	2	16.55	1.8	137.6	10.76	1.6
	A5	110.2	6.63	0.197	33.7	46.8	6.5	0.40	138.6	69.4	2	16.55	4.2	137.6	25.76	3.9
	A6	110.2	6.63	0.197	33.7	46.1	6.5	0.29	91.3	46.4	2	16.55	2.8	137.6	17.21	2.6
	C1	110.2	8.63	0.248	34.8	44.2	5.7	0.20	100.7	49.6	2	28.05	1.8	102.3	18.98	2.2
	C2	110.2	8.63	0.248	34.8	43.9	7.3	0.20	110.3	61.4	2	28.05	2.2	102.3	23.49	2.7

bound on the slip strength. The portion of the applied load that is transferred to the concrete core, $V'_{applied}$, is computed using Equation 9, which assumes secant stiffnesses based on the material strengths. Equation 9 is equivalent to provisions in the AISC *Specification* (AISC, 2010) that specify how much load is transferred to the concrete when all of the specimens have compact members:

$$V'_{applied} = P_{applied}\left(1 - \frac{A_s F_y}{A_s F_y + C_2 A_c f'_c}\right) \quad (9)$$

where

$C_2 = 0.85$ for RCFT and 0.95 for CCFT

The nominal bond strength based on current design provisions (AISC, 2010) is tabulated for each of the specimens and is used and along with $V'_{applied}$ to compute the test-to-predicted ratio (Tables 5 and 6). The current design provisions are seen to be very conservative for these specimens, with test-to-predicted ratios ranging from 1.2 to 5.1 for RCFTs and 1.8 to 4.2 for CCFTs, especially when noting that these ratios are a lower bound because few specimens exhibited a failure mode that included slip.

Effective Bond Transfer Length

The transfer length, the length along the column where significant bond stresses occur, varies with material and geometric properties of the CFT and increases with applied load. The length used in the bond strength formula must address two types of slip limit states. The first is slip along the entire length of the column, where, depending on the boundary conditions, a push-out type failure could occur. The second is slip occurring locally, near the point of load application. This type of slip failure is enabled by the formation of a plastic mechanism in either the steel tube or concrete core, allowing the relative motion. Other, more localized failure modes that include slip (e.g., failure of one face of a CFT column where load is framing in) should be addressed in connection design and are not discussed here.

The CFT connection tests provide some insight into an appropriate bond length. The transfer length at peak load, $L_{transfer}$, is computed for the CFT connections tests (Tables 5 and 6) using Equation 10, where p is the entire perimeter of the steel–concrete interface and F_{in} is the critical bond stress, as computed using Equation 6 for RCFTs and Equation 8 for CCFTs:

$$L_{transfer} = \frac{V'_{applied}}{p F_{in}} \quad (10)$$

Use of the formula for bond stress from push-out tests without shear tabs for RCFT (Equation 4) would result in transfer lengths approximately twice as large and could be justified because Equation 4 is recommended for design. However, the formula for bond stress from push-out tests with shear tabs is used for RCFTs, because it is a more accurate assessment for these specimens. The tabulated transfer lengths are of approximately the same magnitude as the lengths over which slip occurred, as reported by the researchers.

In Tables 5 and 6, the transfer length is seen to have a strong correlation with the ratio of load applied at the connection to total load, β (Figure 2). This is due to the fact that the specimens failed at loads near the cross-section strength, thus the specimens with larger β values had larger transferred loads at failure because a larger portion of the load was applied at the connection. The other specimens, with lower β values, presumably could have achieved the similar transferred loads at failure had a greater portion of the load been applied at the connection. Accordingly, the transfer length in Tables 5 and 6 should be considered a lower bound. The ratio of transfer length to tube width for specimens with a large proportion of the load applied at the connection ranges from 2.3 to 4.1 ($\beta \geq 0.4$; Table 5: specimens A1, A2, A3, B2, C1, D1, D2, D3 and D4 by Dunberry et al., 1987; Table 6: specimen A5 by Shakir-Khalil, 1993a). Based on these data, the current provisions for bond length for the case of load applied to the steel tube and the CFT extending to both sides of the point of force transfer (i.e., $C_{in} = 4$) (AISC, 2010) appear to be appropriate and safe for design.

While the CFT connection tests provide valuable information, they are limited by a lack of variety in geometric and material properties and loading configurations and because most specimens did not exhibit a slip related failure. A mechanistic analysis allows exploration of the effective bond transfer length for the range of properties and configurations seen in practice. A suitable bond length would account for both slip limit states: slip along the entire length and localized slip accompanied with overstressing and formation of a plastic mechanism in the steel tube or concrete core.

The normalized length (*L/H* for RCFT or *L/D* for CCFT) of the CFT push-out tests examined in this work varied from 1 to 6. The CFT connections tests exhibited normalized transfer lengths within the same range. While no definite trends were identified in the CFT push-out test results between the normalized length and bond stress, the bond stress as derived from the push-out tests may not be active along the entire length for longer columns. Thus, utilizing the entire length of the column to assess bond strength (i.e., $L_{bond} = L$, extending from mid-height of the column above the connection to mid-height of the column below the connection) may be inappropriate even for the case of slip occurring along the entire length of the column.

For localized slip, the length of the column that slips is relatively small, but to enable this failure mode, a plastic

mechanism needs to develop in either the steel tube or concrete core (depending on where the load is applied). The applied force required to develop the plastic mechanism assuming strengths consistent with current provisions (AISC, 2010) is given in Equation 11a for the case of load applied to the steel tube and the CFT extending to both sides of the point of force transfer, Equation 11b for the case of load applied to the steel tube and the CFT extending to only the compressive side of the point of force transfer, and Equation 11c for the case of load applied to the concrete core regardless of which sides the CFT extends.

$$P_{applied} = A_s F_{cr} + A_s F_y \tag{11a}$$

$$P_{applied} = A_s F_{cr} \tag{11b}$$

$$P_{applied} = C_2 A_c f'_c \tag{11c}$$

where F_{cr} is the critical compressive stress of the steel tube ($F_{cr} \leq F_y$) (AISC, 2010).

Note that when load is applied to the steel tube and the CFT extends to both sides, the compressive strength on one side and the tensile strength on the other side need to be met simultaneously to form a plastic mechanism. Thus, depending on the proportioning of the section, this limit state may be precluded by the cross-section strength of the composite column.

To determine an appropriate value for the bond length when a localized overstressing failure controls, the transfer length is computed when the applied load is equal to the limit (Equation 11). The transfer length is computed using Equation 12a for the case of load applied to the steel tube and Equation 12b for the case of load applied to the concrete core. These equations are as given in the AISC *Specification* (AISC, 2010), with the exception that F_{cr} is used instead of F_y to determine the portion of the load supported by the steel tube. This change was necessary to yield realistic results for slender tubes. Note that $F_{cr} = F_y$ in the controlling cases presented here; thus, this deviation from the AISC *Specification* has no effect on the proposed recommendations.

$$P_{applied}\left(1 - \frac{A_s F_{cr}}{P_{no}}\right) = pF_{in}L_{transfer} \tag{12a}$$

$$P_{applied}\left(\frac{A_s F_{cr}}{P_{no}}\right) = pF_{in}L_{transfer} \tag{12b}$$

where P_{no} is the nominal compressive strength of zero length CFT (AISC, 2010).

The computed transfer length is normalized by the outside dimension of the steel tube (H for RCFT; D for CCFT) to be comparable with the parameter C_{in}. The minimum normalized transfer lengths for practical ranges of material parameters ($F_y \geq 36$ ksi, $E_s = 29{,}000$ ksi, $f'_c \geq 3$ ksi) and geometric parameters ($H \geq 4$ in., $H/B \leq 2$, $B/t \geq 10$, $H/t \leq 400$ for RCFT; $D \geq 4$ in., $10 \leq D/t \leq 400$ for CCFT) and only for cases where the plastic mechanism was not precluded by the cross-section strength are presented in Table 7 for RCFTs and Table 8 for CCFTs for the various configurations. Based on these results, an appropriate value for C_{in} in the bond strength equation is 4 for the case of load applied to the steel tube and the CFT extending to both sides of the point of force transfer and 2 otherwise. The value of 4 for the case of load applied to the steel tube and steel tube and the CFT extending to both sides of the point of force transfer is in agreement with results of the CFT connection tests described earlier; there is no experimental evidence for the other configurations. These recommendations regarding C_{in} represent a minor change from the current provisions, where $C_{in} = 4$ when the CFT extends to both sides of the point of force transfer regardless of whether the load is applied to the steel or to the concrete. It is further recommended that in cases where the nominal bond length ($C_{in}H$ for RCFTs; $C_{in}D$ for CCFTs) of adjacent connection regions overlaps (e.g., columns with a low length-to-depth ratio or with beams framing in a staggered pattern), the bond length should be taken as a reduced value computed such that no overlap occurs.

An alternative form of the bond length could include the height of the shear tab. This form would have the advantage of being more consistent with the definition of the load transfer region used for detailing shear connectors in composite columns (AISC, 2010). If such a form was chosen, the value of C_{in} would need to be adjusted accordingly.

Effective Bond Transfer Width

Current design provisions in the AISC *Specification* allow only a portion of the perimeter of the steel–concrete interface to be used when computing the transfer strength (AISC, 2010). This is unique among the existing and proposed design provisions examined in this paper (Tomii, 1985; Roeder et al., 1999; Parsley et al., 2000; CEN, 2004). Based on observations of friction marks on tested and disassembled push-out specimens, Shakir-Khalil (1993b) noted that for CCFTs the entire perimeter is engaged in bond transfer, whereas for RCFTs only the corner regions participate. There is limited evidence regarding the portion of the width that is active when various numbers of girders frame into either a CCFT or a RCFT column because the majority of tests have been completed with two girders. The CFT

Table 7. RCFT Minimum Transfer Lengths from Mechanistic Analysis									
Case		H (in.)	B (in.)	t (in.)	H/t	F_y (ksi)	f'_c (ksi)	$L_{transfer}$ (in.)	$L_{transfer}/H$
Square CFT	Load on steel, column extends both sides	4.00	4.00	0.067	59.5	36.0	3.0	48.43	12.11
	Load on steel, column extends below only	4.00	4.00	0.132	30.3	36.0	3.0	16.06	4.02
	Load on concrete	4.00	4.00	0.132	30.3	36.0	3.0	16.06	4.02
RCFT	Load on steel, column extends both sides	4.00	4.00	0.067	59.5	36.0	3.0	48.43	12.11
	Load on steel, column extends below only	6.96	4.00	0.400	17.4	36.0	3.0	22.91	3.29
	Load on concrete	6.96	4.00	0.400	17.4	36.0	3.0	22.91	3.29

Table 8. CCFT Minimum Transfer Lengths from Mechanistic Analysis							
Case	D (in.)	t (in.)	D/t	F_y (ksi)	f'_c (ksi)	$L_{transfer}$ (in.)	$L_{transfer}/D$
Load on steel, column extends both sides	4.00	0.075	53.5	36.0	3.0	19.13	4.78
Load on steel, column extends below only	4.00	0.104	38.4	36.0	3.0	7.94	1.99
Load on concrete	4.00	0.104	38.4	36.0	3.0	7.94	1.99

connection tests conducted by Shakir-Khalil and Al-Rawdan (1995) with only one girder framing in had experienced lower transfer loads than the other specimens (Table 5), but it is important to note that the specimen did not suffer a bond failure and would likely have resisted higher transfer loads if the specimen were designed to mitigate non-slip-related failure. The experimental bond stress for push-out tests, including those with shear tabs, is computed assuming the full perimeter is engaged in slip. All of the push-out tests with shear tabs in Tables 3 and 4 have two girders framing on opposite sides. This implies that, for columns with at least two girders framing in on opposite sides, the bond stress can be achieved for the entire perimeter. For the cases of edge and corner columns where one girder or two girders on adjacent sides frame in, it is unclear whether or not the entire perimeter is engaged. However, these configurations will induce bending moments into the columns, thus increasing the bond strength. Therefore, using the entire perimeter for corner columns is likely justified and is proposed for use in this work.

PROPOSED DESIGN FORMULA

Based on the preceding analyses of critical bond stress, longitudinal bond transfer length and circumferential bond transfer width, the formula for nominal bond strength is proposed as:

(a) For RCFT:

$$R_n = 2\left(B+H\right)L_{bond}F_{in} \tag{13a}$$

$$L_{bond} = C_{in}H \tag{13b}$$

$$F_{in} = 12.1\left(t/H^2\right) \le 0.1 \tag{13c}$$

(b) For CCFT:

$$R_n = \pi D L_{bond}F_{in} \tag{14a}$$

$$L_{bond} = C_{in}D \tag{14b}$$

Table 9. Computation of Resistance and Safety Factors					
Type	Number of Experiments	R_m/R_n	V_R	ϕ	Ω
RCFT	18	0.91	0.43	0.45	3.37
CCFT	127	1.26	0.51	0.55	2.74

$$F_{in} = 30.7\left(t/D^2\right) \leq 0.2 \quad (14c)$$

where

R_n = nominal bond strength, kips
F_{in} = nominal bond stress, ksi
t = design wall thickness of steel section, in.
B = overall width of rectangular steel section ($B \leq H$), in.
H = overall height of rectangular steel section ($H \geq B$), in.
D = outside diameter of round steel section, in.
L_{bond} = length of the bond region (the bond region of adjacent connections shall not overlap)
C_{in} = 4 if load is applied to the steel tube and the CFT extends to both sides of the point of force transfer
= 2 otherwise

For simplicity in design, the perimeter of the steel–concrete interface is approximated using the outside dimensions of the steel tube (i.e., $p = 2(B + H)$ for RCFT and $p = \pi D$ for CCFT). The error introduced from this simplification is small in comparison to the scatter in the results.

An upper bound is placed on the bond stress based on the bond stress observed in experimental results of the stockiest tubes for each shape. For very large cross-sections and thin steel tubes, the bond stress approaches zero, essentially requiring an alternate force transfer mechanism when significant loads are applied.

The proposed formula differs from the current formula (AISC, 2010) in the bond strength, bond length, and bond width. In the proposed equation, the bond width is the entire perimeter of the interface, regardless of the number of girders framing in. The resulting strength should be compared against the force transfer demand from all girders framing in, as opposed to checking each girder individually as implied by the current design formula (AISC, 2010).

The proposed formula for bond stress is based on geometric properties of the tube only. It is noted that concrete quality (e.g., the shrinkage/expansive potential) also affects the bond stress. This was not included in the proposed formula because the concrete quality is not typically known at the time of design. However, higher and more reliable bond strengths could be obtained if there were requirements placed on the quality of the concrete (Roeder et al., 1999).

To compute a resistance factor for load and resistance factor design, the recommendations of Ravindra and Galambos (1978) are used. The proposed formula for the resistance factor (Equation 15) depends on the desired reliability index, β_o; coefficient of variation of the resistance, V_R; and the mean test-to-predicted ratio, R_m/R_n:

$$\phi = \frac{R_m}{R_n} e^{(-0.55\beta_o V_R)} \quad (15)$$

Unfortunately, no suitable set of tests exists to compute reliable statistics on the resistance or test-to-predicted ratio for the bond strength. The CFT connection tests results have unnaturally high variation because the peak applied loads do not always reflect bond failures (i.e., other failure modes govern the peak strength). An approximate result can be obtained by computing the resistance factor for the bond stress. The nominal bond stress given by Equations 13b and 14b is compared to the experimentally observed bond stress for the specimens in Tables 1 and 2. The resulting mean and coefficient of variation of the test-to-predicted ratio are presented in Table 9. In this case, only uncertainty from the bond stress will be included. Assuming a reliability index of 3.0, as is recommended for members (Ravindra and Galambos, 1978), the resistance factor is computed as 0.45 for RCFT and 0.55 for CCFT. A value of 0.45 is recommended for both shapes. The corresponding safety factor for allowable stress design is computed as 3.33 ($\Omega = 1.5/\phi$). These values are consistent with those in the current AISC *Specification* (2010).

DISTRIBUTION OF BOND STRESS ALONG COLUMN HEIGHT

The current (AISC, 2010) and the proposed design equations assume that the bond stress is uniform over a given height of the column. However, distribution of bond stress is known to vary both along the perimeter of the interface and along the height of the columns. This complex three-dimensional behavior is most accurately analyzed using detailed continuum finite element models (Roeder et al., 1999; Johansson, 2003). One-dimensional analysis, assuming constant behavior around the perimeter of the interface, complements the more detailed analyses and provides a valuable link between the complex three-dimensional behavior and

simple design equations. The derivation presented here is essentially a simple case of the bond model developed by Hajjar et al. (1998), applicable only to concentrically loaded columns with negligible geometric nonlinearity. This section thus assesses the nonlinear distribution of bond stress using one-dimensional analysis and justifies the use of a uniform bond stress in design calculations.

The distribution of bond stress along the height of the column depends on the response of the steel tube and the concrete core, as well as the interface between the two. A differential equation can be formed to describe the slip behavior by assessing equilibrium on an infinitesimal length of a CFT column. A free-body diagram of the CFT segment is shown in Figure 5. Equilibrium can be assessed for the steel and concrete components (Equation 16):

$$\Sigma F_{concrete} = A_c\sigma_c(x) - A_c\sigma_c(x+dx) - p\,dx\,\tau(x) = 0 \quad (16a)$$

$$\Sigma F_{steel} = A_s\sigma_s(x) - A_s\sigma_s(x+dx) + p\,dx\,\tau(x) = 0 \quad (16b)$$

where

A_s = cross-sectional area of the steel tube
A_c = cross-sectional area of the concrete core
p = perimeter of the steel–concrete interface
x = variable defined by the length along the CFT
dx = length of the segment of CFT analyzed (Figure 5)
$\sigma_s(x)$ = longitudinal stress in the steel tube
$\sigma_c(x)$ = longitudinal stress in the concrete core
$\tau(x)$ = bond stress

If elastic behavior is assumed (i.e., steel and concrete stresses are linear functions of strain and bond stress is a linear function of slip), the general solution of the resulting differential equation is Equation 17 (Denavit, 2012).

$$\tau(x) = C_1e^{Cx} + C_2e^{-Cx} \quad (17)$$

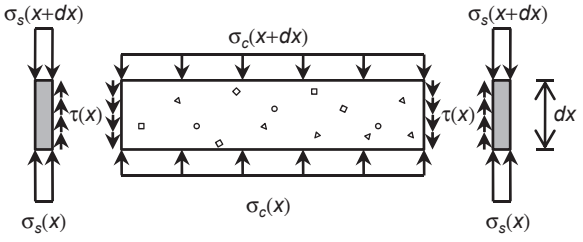

Fig. 5. Free-body diagram of CFT section.

where

$$C = \sqrt{\frac{p\kappa}{E_cA_c} + \frac{p\kappa}{E_sA_s}}$$

E_s = elastic modulus of the steel tube
E_c = elastic modulus of the concrete core
κ = elastic stiffness of the bond-slip relation
C_1 and C_2 = constants that depend on boundary conditions

The specific solution depends on the boundary conditions of the column. One representative case—one side of a shear connection where the peak bond stress is just reached and the column is of sufficient length to completely transfer the load—will be examined further. The boundary conditions for this case can be described by Equation 18:

$$\tau(0) = F_{in} \quad \tau(\infty) = 0 \quad (18)$$

Solving for the constants, the distribution of the bond stress is described by Equation 19. The equation indicates that the bond stress exponentially decays away from the point of load applications. The force transfer between materials persists along the full length of the column, although after a relatively short distance the bond stress is negligibly small. This behavior has been noted previously in analyses performed by Roeder et al. (1999).

$$\tau(x) = F_{in}e^{-Cx} \quad (19)$$

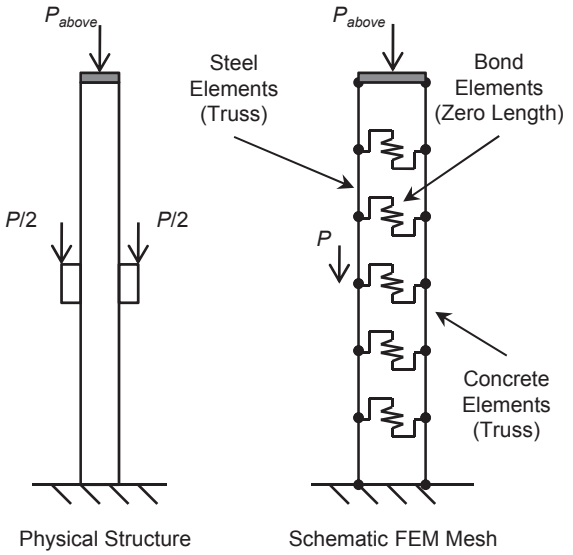

Fig. 6. Schematic of FEM mesh.

The load transferred can be computed by integrating along the length of the column and is found to be pF_{in}/C.

Examining the elastic behavior gives insight into the distribution of bond stress; however, nonlinearity in the steel tube, concrete core and bond behavior is expected at the ultimate limit state. A material nonlinear analysis was conducted using existing structural analysis formulations, noting that the governing differential equations can be modeled with two strands of linked truss elements. The steel tube and concrete core are modeled with truss elements, and the interface is modeled with zero length springs located at the nodes. This configuration is shown schematically in Figure 6. Typically, 200 elements along the length of the column were used in the analyses; the large number of elements provided for smooth results along the length of the column. When elastic materials are used, the analytical results (Equation 18) are captured exactly by this computational model. Suitable uniaxial material models have been developed in previous studies for RCFT (Tort and Hajjar, 2010) and CCFT (Denavit and Hajjar, 2012). An elastic–perfectly plastic model is used to describe the load-slip relationship with peak stress computed by Equation 13b for RCFT and Equation 14b for CCFT and the initial stiffness taken as 66 kip/in^3, based on recommendations by Hajjar et al. (1998).

Analyses were performed on column segments representing half the story height above and below a simple connection. Slip was constrained to be zero at the top and bottom of the column segment so that the introduction of load at the connection could be investigated without any influence of slip elsewhere in the column. The columns were subjected to a load applied at the top representing load in the column from upper stories and a load applied at the connection (midheight of the segment) equal to the nominal bond strength (Equation 13a for RCFTs and Equation 14a for CCFTs). Results include the distribution of slip, bond stress and axial load in the steel tube and concrete core along the height of the column. Sample results from one analysis are shown in Figure 7 for a 10-ft-long segment of a CCFT column constructed from an HSS 7.500×0.250 (F_y = 42 ksi, t_{design} = 0.233 in, F_{in} = 127.2 psi) and normal-strength concrete (f'_c = 4 ksi). A load of 74.2 kips ($0.2P_{no}$) was applied at the top, and a load of 211.9 kips was applied at the connection.

The horizontal dashed lines denote the nominal bond length ($C_{in}D$) in which the bond stress is assumed active in the design formulation. The nonlinear analysis confirms that the majority of the force transfer occurs in this region, although not all, with some slip extending both above and below this region. The distribution of slip is not symmetric about the connection, with the equilibrium achieved in a shorter length below the connection than above. This is due to the gradual decrease in stiffness of the steel tube and concrete core as loads are increased. The variation in stiffness with loading is also seen in the load sharing in the equilibrium regions. Above the connection the steel carries 52% of the axial load, while below the connection the steel carries 60% of the axial load. The percentage below the connection is in agreement with the AISC *Specification* (Equation 9), but because the percentage above is lower, the transferred

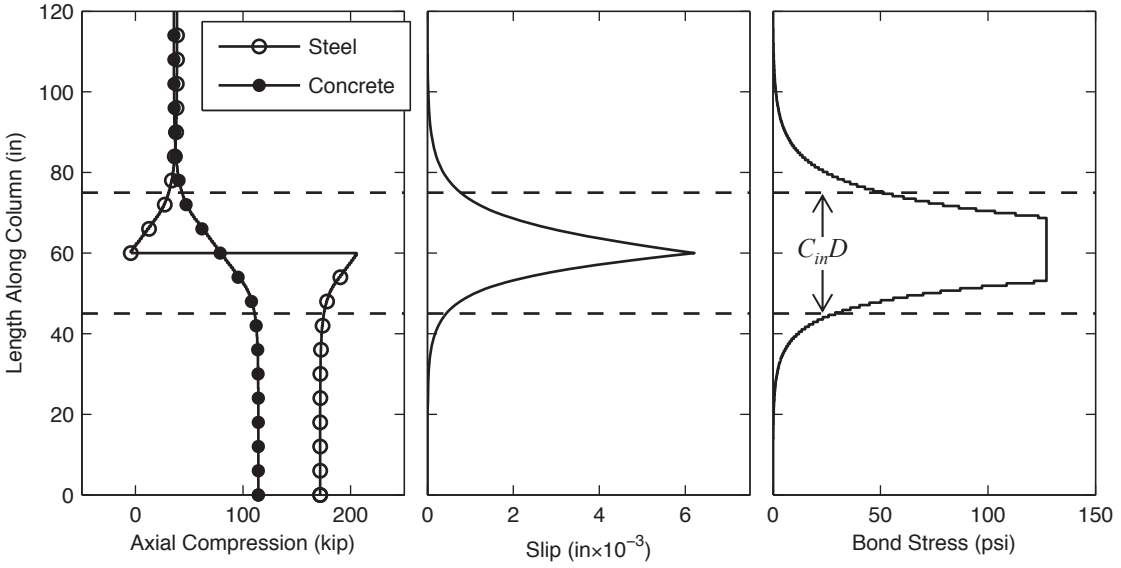

Fig. 7. Sample results of nonlinear bond analysis.

load is slightly underpredicted. The magnitude of slip at the nominal bond strength is rather small (on the order of one-hundredth of an inch), confirming that natural bond strength should not be superimposed with other force transfer mechanisms that may not develop their full strength at these low levels of deformation.

CONCLUSIONS

Current design provisions for the natural bond strength are overly simple and are found to be conservative for the cases examined. A new formula for nominal bond strength of CFT structures is proposed in this paper. The critical bond stress, given as a function of tube dimensions, is derived from results of push-out test and varies between RCFT and CCFT. The effective bond transfer area is determined based on an examination of experimental observations and results from specially instrumented connection tests. The resistance factor is computed as 0.45, and the safety factor is computed as 3.33, based on the bond stress formula. Using a one-dimensional model, the behavior of the connection region of a column was examined. The distribution of bond stress and the load deformation response at the joint both indicate that the proposed design formula is safe.

Finally, it is noted that because the proposed formula is based on experimental results that do not generally exhibit a bond slip failure, there is a degree of conservatism in the design recommendations. Thus, future experimental and analytical research is warranted to explore the behavior of CFT columns subjected large transfer forces.

NOTATION

A_c, A_s	Cross-sectional area of the concrete and steel
B	Overall width of rectangular steel section ($B \leq H$)
C	Constant in bond stress formula (Equation 16)
C_{in}	Coefficient for longitudinal bond height
D	Outside diameter of round steel section
E_c, E_s	Modulus of elasticity of the concrete and steel
F_{cr}	Critical compressive stress of the steel ($F_{cr} \leq F_y$)
F_{in}	Nominal bond stress
F_y	Steel yield strength
H	Overall height of rectangular steel section ($H \geq B$)
L	Specimen length
L_{bond}	Length used when determining bond strength
$L_{transfer}$	Length along the column where significant bond stresses occur
$P_{applied}$	Applied force
P_{no}	Nominal CFT section compressive strength
R_n	Nominal bond strength
$V'_{applied}$	Portion of applied force that is transferred
d_c, d_s	Displacement of the concrete and steel
f'_c	Concrete compressive strength
p	Perimeter of the steel–concrete interface
s	Slip
t	Thickness of steel tube
Ω	Safety factor
β	Applied load ratio
ϕ	Resistance factor
κ	Bond stiffness
σ_c, σ_s	Longitudinal stress of the concrete and steel
τ	Shear stress at steel–concrete interface

ACKNOWLEDGMENTS

Funding for this research was provided by the National Science Foundation under Grant No. CMMI-0619047, the American Institute of Steel Construction, the National Natural Science Foundation of China (90815029, 51021140006), China Scholarship Council (2007102420) and the University of Illinois at Urbana-Champaign. The authors thank Steven Palkovic, Matthew Eatherton and Luis Pallarés for their assistance with this research.

REFERENCES

AISC (2010), *Specification for Structural Steel Buildings*, ANSI/AISC 360-10, American Institute of Steel Construction, Chicago, IL.

Aly, T., Elchalakani, M., Thayalan, P. and Patnaikuni, I. (2010), "Incremental Collapse Threshold for Pushout Resistance of Circular Concrete Filled Steel Tubular Columns," *Journal of Constructional Steel Research*, Vol. 66, No. 1, pp. 11–18.

Bridge, R. and Webb, J. (1993), "Thin Walled Circular Concrete Filled Steel Tubular Columns," *Composite Construction in Steel and Concrete II*, American Society of Civil Engineers, New York, pp. 634–649.

CEN (2004), *Eurocode 4: Design of Composite Steel and Concrete Structures*, EN1994-1-1, European Committee for Standardization, Brussels, Belgium.

Denavit, M.D. (2012), "Characterization of Behavior of Steel–Concrete Composite Members and Frames with Applications for Design," Ph.D. Dissertation, Department of Civil and Environmental Engineering, University of Illinois at Urbana–Champaign, Urbana, IL.

Denavit, M.D. and Hajjar, J.F. (2012), "Nonlinear Seismic Analysis of Circular Concrete-Filled Steel Tube Members and Frames," *Journal of Structural Engineering*, ASCE, Vol. 138, No. 9, pp. 1089–1098.

Dunberry, E., LeBlanc, D. and Redwood, R.G. (1987), "Cross-Section Strength of Concrete-Filled HSS Columns at Simple Beam Connections," *Canadian Journal of Civil Engineering*, Vol. 14, No. 2, pp. 408–417.

Hajjar, J.F., Schiller, P.H. and Molodan, A. (1998), "A Distributed Plasticity Model for Concrete-Filled Steel Tube Beam-Columns with Interlayer Slip," *Engineering Structures*, Vol. 20, No. 8, pp. 663-676.

Johansson, M. (2003), "Composite Action in Connection Regions of Concrete-Filled Steel Tube Columns," *Steel & Composite Structures*, Vol. 3, No. 1, pp 47–64.

Morishita, Y., Tomii, M. and Yoshimura, K. (1979a), "Experimental Studies on Bond Strength in Concrete Filled Circular Steel Tubular Columns Subjected to Axial Loads," *Transactions of the Japan Concrete Institute*, Vol. 1, pp. 351–358.

Morishita, Y., Tomii, M. and Yoshimura, K. (1979b), "Experimental Studies on Bond Strength in Concrete Filled Square and Octagonal Steel Tubular Columns Subjected to Axial Loads," *Transactions of the Japan Concrete Institute*, Vol. 1, pp. 359–366.

Parsley, M.A., Yura, J.A. and Jirsa, J.O. (2000), "Push-Out Behavior of Rectangular Concrete-Filled Steel Tubes," *Composite and Hybrid Systems*, ACI SP-196, American Concrete Institute, Farmington Hills, MI, pp. 87–107.

Ravindra, K.M. and Galambos, V.T. (1978), "Load and Resistance Factor Design for Steel," *Journal of Structural Division*, ASCE, Vol. 104, No. ST9, pp. 1337–1353.

Roeder, C.W., Cameron, B. and Brown, C.B. (1999), "Composite Action in Concrete Filled Tubes," *Journal of Structural Engineering*, ASCE, Vol. 125, No. 5, pp. 477–484.

Roeder, C.W., Lehman, D.E., and Thody, R. (2009), "Composite Action in CFT Components and Connections," *Engineering Journal*, AISC, Vol. 46, No. 4, pp. 229–242.

Shakir-Khalil, H. (1991), "Bond Strength in Concrete-Filled Steel Hollow Sections," *International Conference on Steel and Aluminum Structures*, Singapore, May 22–24, pp. 157–168.

Shakir-Khalil, H. (1993a), "Full-Scale Tests on Composite Connections," *Composite Construction in Steel and Concrete II*, American Society of Civil Engineers, New York, pp. 634–649.

Shakir-Khalil, H. (1993b), "Pushout Strength of Concrete-Filled Steel Hollow Sections," *The Structural Engineer*, Vol. 71, No. 13, pp. 230–233.

Shakir-Khalil, H. (1993c), "Resistance of Concrete-Filled Steel Tubes to Pushout Forces," *The Structural Engineer*, Vol. 71, No. 13, pp. 234–243.

Shakir-Khalil, H. (1993d), "Connection of Steel Beams to Concrete-Filled Tubes," *Proc. 5th International Symposium on Tubular Structures*, Nottingham, England, UK, August 25–27, pp. 195–203.

Shakir-Khalil, H. (1994a), "Finplate Connections to Concrete-Filled Tubes," *Proc. 4th International Conference on Steel-Concrete Composite Structures*, Kosice, Slovakia, June 20–23, pp. 181–185.

Shakir-Khalil, H. (1994b), "Beam Connections to Concrete-Filled Tubes," *Proc. 6th International Symposium on Tubular Structures*, Melbourne, Australia, December 14–16, pp. 357–364.

Shakir-Khalil, H. and Al-Rawdan, A. (1995), "Behavior of Concrete-Filled Tubular Edge Columns," *Proc. 3rd International Conference on Steel and Aluminum Structures*, Istanbul, Turkey, May, pp. 515–522.

Tomii, M. (1985), "Bond Check for Concrete-Filled Steel Tubular Columns," *Composite and Mixed Construction*, American Society of Civil Engineers, New York, pp. 195–204.

Tomii, M., Yoshimura, K. and Morishita, Y. (1980a), "A Method of Improving Bond Strength Between Steel Tube and Concrete Core Cast in Square and Octagonal Steel Tubular Columns," *Transactions of the Japan Concrete Institute*, Tokyo, Vol. 2, pp. 327–334.

Tomii, M., Yoshimura, K. and Morishita, Y. (1980b), "A Method of Improving Bond Strength Between Steel Tube and Concrete Core Cast in Circular Steel Tubular Columns," *Transactions of the Japan Concrete Institute*, Tokyo, Vol. 2, pp. 319–326.

Tort, C. and Hajjar, J. F. (2010), "Mixed Finite-Element Modeling of Rectangular Concrete-Filled Steel Tube Members and Frames under Static and Dynamic Loads," *Journal of Structural Engineering*, ASCE, Vol. 136, No. 6, pp. 654–664.

Virdi, K.S. and Dowling, P.J. (1980), "Bond Strength in Concrete Filled Steel Tubes," *IABSE Periodical*, August, pp. 125–139.

Xu, C., Chengkui, H., Decheng, J. and Yuancheng, S. (2009), "Push-Out Test of Pre-Stressing Concrete Filled Circular Steel Tube Columns by Means of Expansive Cement," *Construction and Building Materials*, Vol. 23, pp. 491–497.

Yin, X. and Lu, X. (2010), "Study on Push-Out Test and Bond Stress-Slip Relationship of Circular Concrete Filled Steel Tube," *Steel and Composite Structures*, Vol. 10, No. 4, pp. 317–329.

ERRATA

Bond Behavior of Concrete-Filled Steel Tube (CFT) Structures

Paper by JIE ZHANG, MARK D. DENAVIT, JEROME F. HAJJAR and XILIN LU

(4th Quarter, 2012)

After this paper had gone to press, it was determined that four specimens were accidentally included twice in the databases for push-out tests without shear tabs. These duplicate specimens have been removed, and two other specimens that were inadvertently excluded have been added. Additionally, for four of the specimens, the measured tube thickness has been included in place of the nominal tube thickness that was reported in the original paper. Tables 1 and 2 have been revised to reflect these corrections.

These corrections result in minor changes to the empirical bond stress formulas, Equations 3, 4, 7, 8, 13c, and 14c, as well as Figure 4, have been revised to reflect the corrections:

$$F_{in} = 1.15\times10^{6}\left(H/t\right)^{-2.90} \quad R^2 = 0.69 \tag{3}$$

$$F_{in} = 12800\left(t/H^2\right) \quad R^2 = 0.62 \tag{4}$$

$$F_{in} = 27900\left(D/t\right)^{-1.59} \quad R^2 = 0.32 \tag{7}$$

$$F_{in} = 30900\left(t/D^2\right) \quad R^2 = 0.50 \tag{8}$$

$$F_{in} = 12.8\left(t/H^2\right) \le 0.1 \tag{13c}$$

$$F_{in} = 30.9\left(t/D^2\right) \le 0.2 \tag{14c}$$

The corrections to the database also result in minor changes to the proposed resistance and safety factors. Table 9 has been updated to reflect the corrections; values of $\phi = 0.50$ and $\Omega = 3.00$ are recommended for both CCFT and RCFT.

The data and formulas were used elsewhere in the paper; however, the resulting changes are slight and do not affect the conclusions. Specifically:

- Equation 8 was used in the computation of the last three columns of Table 6. The original and corrected numbers differ by less than 1%.
- Equations 13c and 14c were used in the mechanistic analysis to determine the minimum transfer lengths presented in Tables 7 and 8. Table 7 has been revised to reflect the corrections. In Table 8, the original and corrected numbers differ by less than 1%. The resulting recommendation for C_{in} has not changed.
- Equation 8 was used to compute the bond stress and the load applied at the connection for the analysis presented in Figure 7. The original and corrected numbers differ by less than 1%. The observations from the analyses have not changed.

Table 1. RCFT Push-Out Tests without Shear Tabs								
Reference	Number of Specimens	L (in.)	H, B (in.)	t (in.)	H/t, B/t	F_y (ksi)	f'_c (ksi)	F_{in} (psi)
Shakir-Khalil, 1993a	10	8–24	3.1–5.9	0.20	16–30	43.0	5.6–5.9	48–193
Shakir-Khalil, 1993b	3	16	5.9	0.20	30	43.0	5.2–5.7	29–61
Parsley et al., 2000	4	48–60	8.0–10.0	0.23	35–43	48.0	5.9–6.5	25–42

Table 2. CCFT Push-Out Tests without Shear Tabs								
Reference	Number of Specimens	L (in.)	D (in.)	t (in.)	D/t	F_y (ksi)	f'_c (ksi)	F_{in} (psi)
Virdi and Dowling, 1975	82	6–18	5.8–12.0	0.22–0.40	15–32	mild steel	3.2–6.7	75–431
Shakir-Khalil, 1993a	6	8–24	6.6	0.20	34	43.0	6.1	95–135
Shakir-Khalil, 1993b	3	16	6.6	0.20	34	43.0	5.6–5.7	63–135
Roeder et al., 1999	18	30–76	10.8–24.0	0.22–0.53	20–109	not given	4.0–6.9	1.5–114
Xu et al., 2009	3	20	6.1–6.3	0.11–0.18	35–57	not given	6.8	87–97
Aly et al., 2010	14	16	4.5	0.13	36	50.8	5.9–13.2	51–181

Table 7. RCFT Minimum Transfer Lengths from Mechanistic Analysis									
	Case	H (in.)	B (in.)	t (in.)	H/t	F_y (ksi)	f'_c (ksi)	$L_{transfer}$ (in.)	$L_{transfer}/H$
Square CFT	Load on steel, column extends both sides	4.00	4.00	0.067	59.5	36.0	3.0	45.78	11.45
	Load on steel, column extends below only	4.00	4.00	0.125	32.0	36.0	3.0	15.80	3.95
	Load on concrete	4.00	4.00	0.125	32.0	36.0	3.0	15.80	3.95
RCFT	Load on steel, column extends both sides	4.00	4.00	0.067	59.5	36.0	3.0	45.78	11.45
	Load on steel, column extends below only	8.00	4.00	0.667	12.0	36.0	3.0	23.12	2.79
	Load on concrete	8.00	4.00	0.667	12.0	36.0	3.0	23.12	2.79

Table 9. Computation of Resistance and Safety Factors					
Type	Number of Experiments	R_m/R_n	V_R	ϕ	Ω
RCFT	17	0.94	0.39	0.50	3.02
CCFT	126	1.27	0.50	0.56	2.70

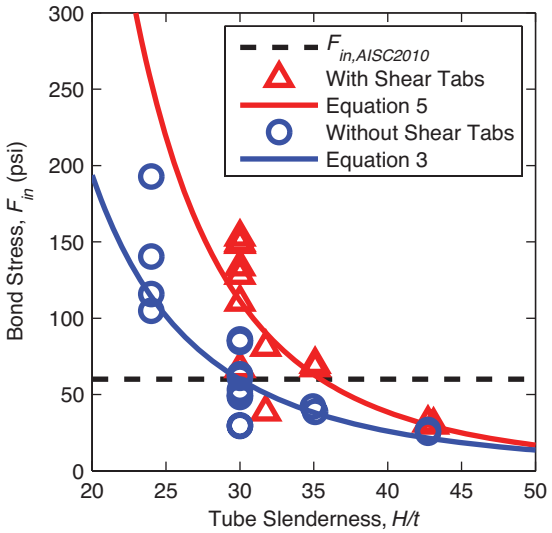

(a) Bond stress of RCFT as a function of H/t

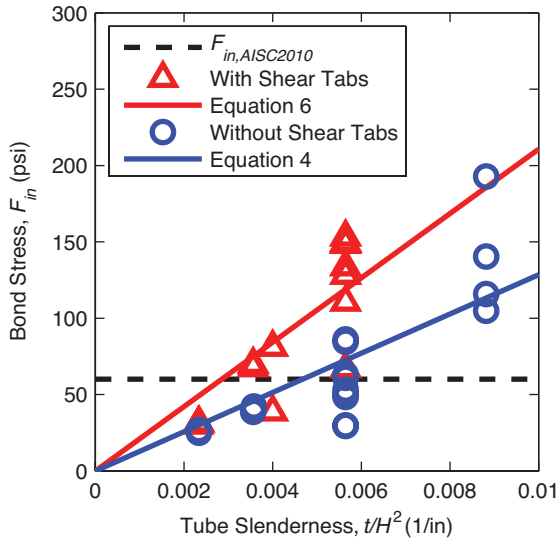

(b) Bond stress of RCFT as a function of t/H^2

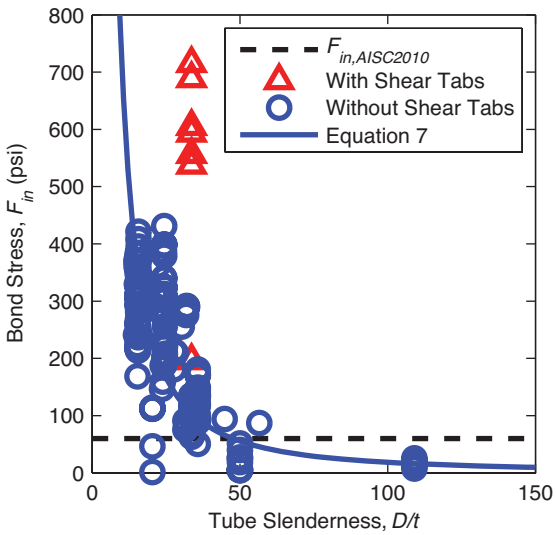

(c) Bond stress of CCFT as a function of D/t

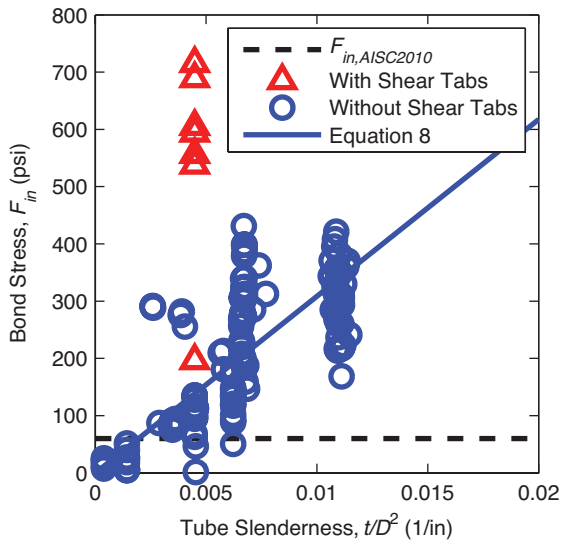

(d) Bond stress of CCFT as a function of t/D^2

Fig. 4. Bond stress for CFT as a function of tube slenderness.